

Bis-Porphyrin-Anthraquinone Triads: Synthesis, Spectroscopy and Photochemistry

Lingamallu Giribabu, P.Silviya Reeta, Ravi Kumar Kanaparthi, Malladi Srikanth, and Yarasi Soujanya

J. Phys. Chem. A, **Just Accepted Manuscript** • DOI: 10.1021/jp312134a • Publication Date (Web): 19 Mar 2013

Downloaded from <http://pubs.acs.org> on March 27, 2013

Just Accepted

“Just Accepted” manuscripts have been peer-reviewed and accepted for publication. They are posted online prior to technical editing, formatting for publication and author proofing. The American Chemical Society provides “Just Accepted” as a free service to the research community to expedite the dissemination of scientific material as soon as possible after acceptance. “Just Accepted” manuscripts appear in full in PDF format accompanied by an HTML abstract. “Just Accepted” manuscripts have been fully peer reviewed, but should not be considered the official version of record. They are accessible to all readers and citable by the Digital Object Identifier (DOI®). “Just Accepted” is an optional service offered to authors. Therefore, the “Just Accepted” Web site may not include all articles that will be published in the journal. After a manuscript is technically edited and formatted, it will be removed from the “Just Accepted” Web site and published as an ASAP article. Note that technical editing may introduce minor changes to the manuscript text and/or graphics which could affect content, and all legal disclaimers and ethical guidelines that apply to the journal pertain. ACS cannot be held responsible for errors or consequences arising from the use of information contained in these “Just Accepted” manuscripts.



Bis-Porphyrin-Anthraquinone Triads: Synthesis, Spectroscopy and Photochemistry

L. Giribabu^{*a}, P. Silviya Reeta^a, Ravi Kumar Kanaparthi^a, Malladi Srikanth^b, Y. Soujanya^b

^a Inorganic & Physical Chemistry Division, CSIR-Indian Institute of Chemical Technology, Habsiguda, Hyderabad-500007, (A.P), India.

^b Molecular Modelling Group, Indian Institute of Chemical Technology, Hyderabad-500067, India.

Abstract

Molecular triads based on *bis*-porphyrin-anthraquinone having azomethine-bridge at the pyrrole- β position have been designed and synthesized. Both free-base **AQ-(H₂)₂** and zinc **AQ-(Zn)₂** triads are characterized by elemental analysis, MALDI-MS, ¹H-NMR, UV-Visible and fluorescence spectroscopy (steady-state and time-resolved) as well as electrochemical method. The absorption spectra of both Soret and Q-bands of the triads are red-shifted by 12-20 nm with respect to their monomer units. The study supported by theoretical calculations manifest that there exists a negligible electronic communication in the ground state between the donor porphyrin and acceptor anthraquinone of these triads. However, interestingly, both the triads exhibit significant fluorescence emission quenching (51-92%) of the porphyrin emission compared to their monomeric units. The emission quenching is attributed to the excited state intramolecular photoinduced electron transfer from porphyrins to anthraquinone. The electron transfer rates (k_{ET}) of these triads are found in the range 1.0×10^8 to 7.7×10^9 s⁻¹ and are found to be solvent dependent.

Key Words: Porphyrin, Anthraquinone, Triad, Intramolecular, Electron transfer, Time-resolved.

Corresponding author: giribabu@iict.res.in, Phone: +91-40-27191724, Fax: +91-40-27160921.

1. Introduction

Photosynthetic reaction centres, which convert solar energy into useful chemical energy, consist of a protein matrix and donor-acceptor redox active pigments. During photosynthesis, the primary electron transfer (ET) step occurs from a porphyrin-based complex¹⁻⁵ and subsequently, the excited porphyrin–base complex donates an electron to (bacterio) chlorophylls or their corresponding dimers and then to bacteriopheophytins and quinone acceptors QA and QB⁶, resulting in a long-lived, charge-separated state. Apart from this, the utmost efficiency with which the chlorophyll-quinone antenna harvest the solar energy has also imparted a special interest in designing a wide variety of efficient porphyrin based solar cells as well.⁷ Numerous model molecules have been reported in the literature for better understanding or mimicking the natural photosynthesis.⁸⁻¹³

Covalently/non-covalently linked porphyrin–quinone donor-acceptor (D-A) molecules have been studied extensively as model compounds for the light-induced charge separation step to get insight into the primary event of the natural photosynthesis.¹⁴⁻¹⁸ Many current investigations are concerned with porphyrin–quinone molecules in order to understand the role of distance, orientation, energetic and medium in determining the rate of intramolecular photoinduced electron transfer (PET).^{19,20} Most of these studies were mainly employed either *through-space* (π - π interactions) and/or *through-bond* (superexchange) mechanism. We are particularly interested in *through-bond* mechanism because the PET in many D–A systems is known to be dominated by *through-bond* interactions.^{17,21-23} One must note that, the spacer between the donor and acceptor play an important role in *through-bond* mechanism. As a part of our continuing interest in studying the PET processes,²⁴⁻²⁶ hereby, we report design, synthesis, spectral (UV-Visible, MALDI-MS and ¹H NMR) and electrochemical characterization of *bis*-porphyrin-anthraquinone based molecular triads. Further, photophysical properties of these newly synthesized azomethine-bridged *bis*-porphyrin-anthraquinone triad **AQ-(H₂)₂** and its zinc derivative **AQ-(Zn)₂** have been studied systematically.

2. Experimental

2.1. Materials.

Commercially available reagents and chemicals were used in the present investigations. Analytical reagent grade solvents were used for synthesis, and distilled laboratory grade

solvents were used for column chromatography. Dry chloroform and dichloromethane were prepared by argon-degassed solvent through activated alumina columns. Nitrogen gas (oxygen-free) was passed through a KOH drying column to remove moisture. Neutral Alumina (mesh 60-325, Brockmann activity1) was used for column purification. All the reactions were carried out under nitrogen or argon atmosphere using dry degassed solvents and the apparatus was shielded from ambient light.

2.2. Synthesis.

5,10,15,20-tetraphenyl porphyrin ($\mathbf{H}_2\mathbf{L}^1$), 5,10,15,20-tetraphenyl porphyrinato zinc(II) (\mathbf{ZnL}^1), 2-formyl-5,10,15,20-tetraphenyl porphyrin ($\mathbf{H}_2\mathbf{L}^2$) and 2-formyl-5,10,15,20-tetraphenyl porphyrinato zinc(II) (\mathbf{ZnL}^2) were synthesized as per the reaction procedures reported in the literature.^{27,28}

2.2.1. Synthesis of free base triad, AQ-(H₂)₂: This compound was synthesized by following Schiff's base reaction. 1,2-diaminoanthraquinone (71.4 mg, 0.39 mmol) and $\mathbf{H}_2\mathbf{L}^2$ (50 mg, 0.07 mmol) were dissolved in 50 ml of dry toluene. The resultant reaction mixture was refluxed for 6 h under inert atmosphere. The solvent toluene was removed under reduced pressure. The obtained solid material was subjected to neutral alumina column and eluted with CHCl₃-Hexane (8:2%, v/v). The solvent front running band was the unreacted $\mathbf{H}_2\mathbf{L}^2$ and the second brown colour band was the desired compound. The solvent was removed under vacuum and recrystallized from CH₂Cl₂-hexane to get desired product in 60% isolated yield. Anal. Calcd. for C₁₀₄H₆₆N₁₀O₂ % (1487.70): C, 83.96; H, 4.47; N, 9.41. Found C, 83.87; H, 4.40; N, 9.35. MALDI-MS (TOF) [C₁₀₄H₆₆N₁₀O₂]⁺: 1486 (10%), [C₁₀₄H₆₆N₁₀O₂ - C₄₆H₃₂N₄]²⁺ 861 (50%). IR: ν_{\max} (KBr)/cm⁻¹ 3459, 2918, 1652, 1584, 1429, 1275. ¹H NMR (CDCl₃, δ ppm): 9.50 (s, 2H); 8.75-8.88 (m, 12H); 8.16-8.35 (m, 18H); 7.65-7.86 (m, 24H); 7.60 (m, 2H); 7.52 (m, 2H); 6.75 (d, 2H), and -2.48 (b, 4H).

2.2.2. Synthesis of zinc triad, AQ-(Zn)₂: This compound was synthesized by following analogous reaction procedure adopted for AQ-(H₂)₂, in which AQ and \mathbf{ZnL}^2 were subjected to a condensation reaction. Anal. Calcd. for C₁₀₄H₆₂N₁₀O₂Zn₂ % (1614.45): C, 77.37; H, 3.87; N, 8.68. Found C, 77.47; H, 3.85; N, 8.655. MALDI-MS (TOF) [C₁₀₄H₆₆N₁₀O₂Zn - C₄₆H₃₂N₄Zn]⁺: 926 (100%). IR: ν_{\max} (KBr)/cm⁻¹ 3455, 2929, 1634, 1521, 1278. ¹H NMR (CDCl₃, δ ppm): 9.63 (s, 2H); 8.83-8.99 (m, 12H); 8.16-8.35(m, 18H); 7.68-7.89 (m, 24H); 7.49 (m, 2H); 7.43 (m, 2H); 6.66 (d, 2H).

2.3. Methods and Instrumentation.

¹H-NMR spectra were recorded on a 500MHz INOVA spectrometer. Cyclic and differential-pulse voltammetric measurements were performed on a PC-controlled electrochemical analyzer (CH instruments model CHI620C). All these experiments were performed with 1 mM concentration of compounds in dichloromethane at a scan rate of 100 mV s⁻¹ in which tetrabutyl ammonium perchlorate (TBAP) is used as a supporting electrolyte as documented in our previous reports.²⁹

2.3.1. Theoretical calculations: Full geometry optimization computations of the **AQ-(H₂)₂** and **AQ-(Zn)₂** triads were carried out with the DFT-B3LYP method using 6-31G* basis set and frequency analysis confirmed that the obtained geometries are to be genuine global minimum structures. All calculations were performed with the Gaussian G03 (d01) package on a personal computer.³⁰

2.3.2. Absorption and fluorescence measurements: The optical absorption spectra were recorded on a Shimadzu (Model UV-3600) spectrophotometer. Concentrations of solutions are ca. to be 1 x 10⁻⁶ M (porphyrin Soret band) and 5 x 10⁻⁵ M (porphyrin Q-bands). Steady-state fluorescence spectra were recorded on a Fluorolog-3 spectrofluorometer (Spex model, Jobin Yvon) for solutions with optical density at the wavelength of excitation (λ_{ex}) \approx 0.05. Fluorescence quantum yields (ϕ) were estimated by integrating the fluorescence bands and by using either [**H₂L¹**] (ϕ = 0.13 in CH₂Cl₂), [**ZnL¹**] (ϕ = 0.036 in CH₂Cl₂) as reference compounds.³¹ Fluorescence lifetime measurements were carried on a picosecond time-correlated single photon counting (TCSPC) setup (FluoroLog3-Triple Illuminator, IBH Horiba Jobin Yvon) employing a picosecond light emitting diode laser (NanoLED, λ_{ex} =405 nm) as excitation source. The decay curves were recorded by monitoring the fluorescence emission maxima of the triads (λ_{em} =650nm). Photomultiplier tube (R928P, Hamamatsu) was employed as the detector. The lamp profile was recorded by placing a scatterer (dilute solution of Ludox in water) in place of the sample. The width of the instrument response function (IRF) was limited by the full width at half maxima (FWHM) of the excitation source, \sim 625 ps at 405 nm. Decay curves were analyzed by nonlinear least-squares iteration procedure using IBH DAS6 (version 2.3) decay analysis software. The quality of the fits was judged by the χ^2 values and distribution of the residuals.

3. Results and Discussion

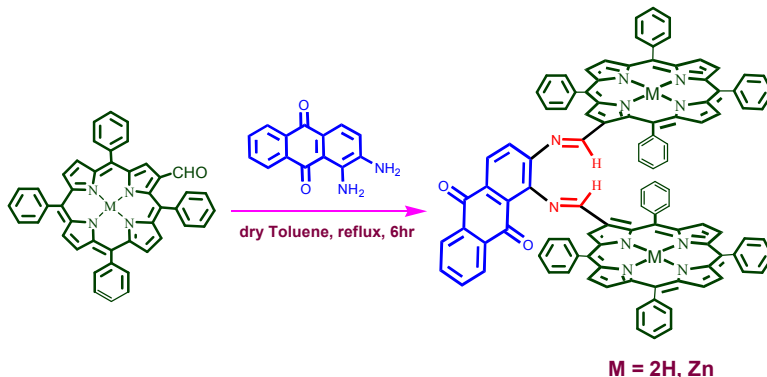


Figure 1: Synthetic scheme of **AQ-(H₂)₂** and **AQ(Zn)₂** triads.

Both the triads **AQ-(H₂)₂** and **AQ(Zn)₂** were synthesized by using Schiff base condensation reaction as shown in Figure 1. The desired compounds were obtained with moderate yields (~ 60%) in both cases after column chromatography purification and subsequent recrystallization. Preliminary characterization of the both triads was carried out by MALDI-TOF MS and UV-Visible spectroscopic methods. The mass spectrum of **AQ-(H₂)₂** showed a peak at $m/z = 1486$ ($[M]^+$, $C_{104}H_{66}N_{10}O_2$) ascribable to the molecular-ion peak. Subsequent peak at $m/z = 861$ can be ascribed to the detachment of one ($[M-C_{104}H_{66}N_{10}O_2 - C_{46}H_{32}N_4]^{2+}$ free-base porphyrin subunit from the triad. A similar type of fragmentation was also observed in case of **AQ-(Zn)₂**. The stretching peak at 1548 & 1521 cm^{-1} in IR spectra of **AQ-(H₂)₂** and **AQ-(Zn)₂**, respectively, conforms the presence of C=N bond in both the triads (**S1&S2**).

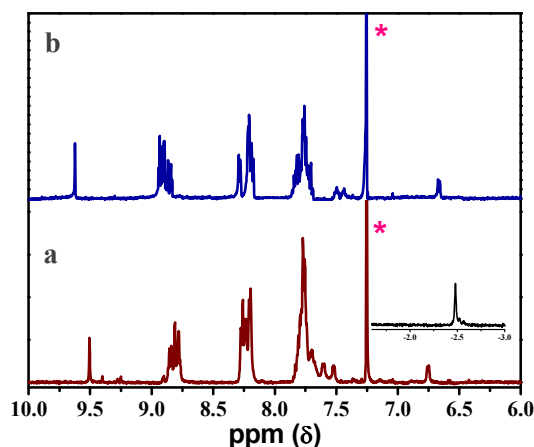


Figure 2: ¹H-NMR spectra of a) **AQ-(H₂)₂** and b) **AQ-(Zn)₂** in $CDCl_3$. The peak labeled with asterisk (*) is due to solvent.

¹H-NMR spectral data of both the triads have been summarized in the experimental section and the spectra of AQ-(H₂)₂ and AQ-(Zn)₂ are shown in Figure 2. Comparison of these spectra with those of individual constituents (H₂L¹, ZnL¹ and AQ) reveals that there is no appreciable change in resonance positions of various protons present on porphyrin macrocycle and that of anthraquinone part of the triad AQ-(H₂)₂, whereas in case of AQ-(Zn)₂, subtle shift of protons probably due to the interaction of anthraquinone part of the triad with zinc porphyrin is observed.¹⁷ This is reasonable if one considers that the two aromatic rings are in ‘*trans*’ configuration with respect to the C=N spacer, avoiding steric interaction. This is confirmed by energy minimization study of the triads which is discussed in section 3.3.

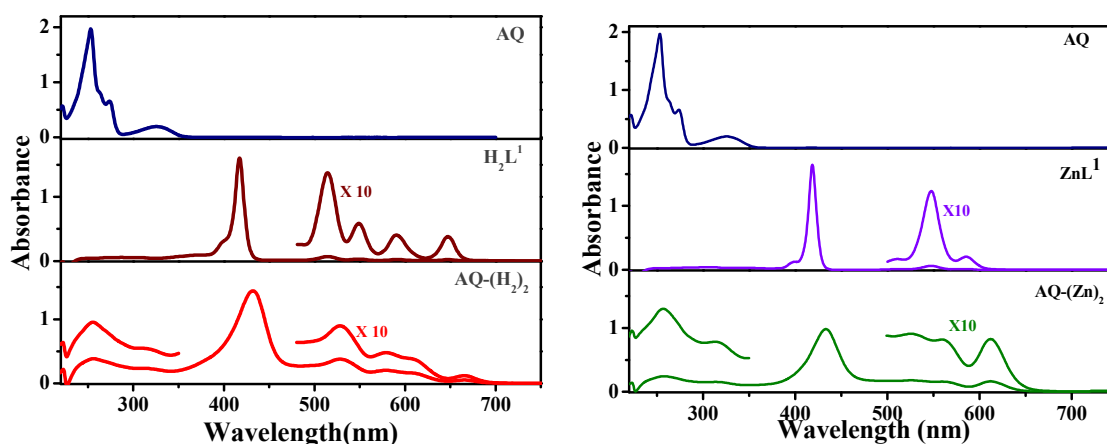


Figure 3: Absorption behaviour of AQ, H₂L¹, AQ-(H₂)₂, ZnL¹ and AQ-(Zn)₂ in CH₂Cl₂.

Table 1: UV-visible and electrochemical data of AQ, H₂L¹, AQ-(H₂)₂ and AQ-(Zn)₂.

Compound	Absorption, λ_{\max} , nm (log ϵ , M ⁻¹ cm ⁻¹) ^a					Potential V vs. SCE ^b		
	Porphyrin Bands					AQ bands	Reduction	Oxidation
H ₂ L ¹	416 (6.06)	515 (4.27)	549 (3.90)	592 (3.77)	646 (3.69)	-	-1.22, -1.56	1.01, 1.25
ZnL ¹	419 (6.17)	547 (4.34)	586 (3.60)			-	-1.45, -1.71	0.72, 1.06
AQ						256 (7.40)	-0.96, -1.38	-
AQ-(H ₂) ₂	433 (5.40)	527 (4.69)	580 (4.39)	608 (4.34)	668 (3.77)	257 (4.91)	-0.86, -1.10, -1.50	1.00, 1.27
AQ-(Zn) ₂	434 (5.6)	526 (4.72)	560 (4.71)	613 (4.72)		257 (4.90)	-0.83, -1.28 -1.54	0.89, 1.21

^aSolvent CH₂Cl₂, Error limits: λ_{\max} , ± 1 nm, $\log \epsilon$, $\pm 10\%$. ^bCH₂Cl₂, 0.1 M TBAP; Glassy carbon working electrode, Standar calomel electrode is reference electrode, Pt electrode is auxillary electrode. Error limits, $E_{1/2} \pm 0.03$ V.

3.1. Ground state properties.

Electronic absorption profile of **AQ-(H₂)₂** and **AQ-(Zn)₂** have been measured in CH₂Cl₂ and the spectral behaviour is compared with individual monomer units, **H₂L¹** and **ZnL¹** (Figure3). Spectroscopic data which include wavelength of maximum absorbance (λ_{\max}), molar extinction coefficients ($\log \epsilon$) of both triads and their constituent individual components are summarized in Table 1. As shown in figure 3, the absorption spectrum is a combination of constituent porphyrin and anthraquinone. Both triads exhibit characteristic intense Soret band (~ 430 nm), which is an $a_{1u}(\pi)/e_g(\pi^*)$ electronic transition, assigned to the second excited state (S_2) and Q-bands (500-700nm) originated from $a_{2u}(\pi)/e_g(\pi^*)$ electronic transition, attributed to the first excited state (S_1). These characteristic bands are similar to many other dimers or trimers.^{32,33} The band centered at ~ 260 nm is largely due the anthraquinone moiety as the porphyrin have very limited/poor absorption at that region (230-350 nm). It is also observed that the bands are red-shifted and slightly broadened compared to simple **H₂L¹** and **ZnL¹** porphyrin units. Similar such red-shifts and broadening were observed in other pyrrole- β substituted porphyrins as well.^{28,34,35} This spectral red-shift (20-30nm) can be explained based on the extended π - electron conjugation of porphyrin unit to the anthraquinone, from there to the other porphyrin unit through the two imine (-C=N-) links. The broadening is more pronounced at the longer wavelength region (>600 nm) which might be due to charge or electron transfer because of donor-acceptor-donor type of molecular arrangement. However, the spectral broadening does not affect further with the solvent polarity indicates the lack of ground state charge or electron transfer (figure S9). So, the broadening which we observe perhaps is due to conformers originated from different orientations of porphyrin units around the two -C-N- bonds.³⁶

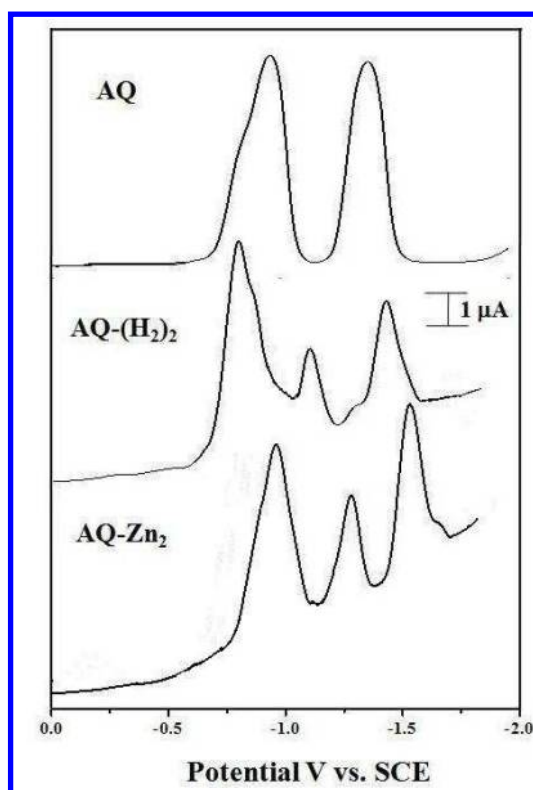


Figure 4: Differential pulse voltammograms of AQ, H_2L^1 , AQ-(H_2)₂ and AQ-(Zn)₂ in CH_2Cl_2 with 0.1 M TBAP.

Figure 4 illustrates the differential pulse voltammograms of AQ, AQ-(H_2)₂ and AQ-(Zn)₂ and Table 1 summarises the redox potential data (CH_2Cl_2 and 0.1 M TBAP) of the D₂-A systems investigated in this study along with that of the corresponding individual constituents. Figure 4 and data in Table 1 indicates that each new compound investigated shows three reduction peaks and two oxidation peaks under the experimental conditions employed in this study. Wave analysis suggested that, in general, while the first two reduction steps and first two oxidation steps are reversible ($i_{pc}/i_{pa} = 0.9-1.0$) and diffusion-controlled ($i_{pc}/\nu^{1/2} = \text{constant}$ in the scan rate (ν) range 50-500 mV/s) one-electron transfer ($\Delta E_p = 60-70$ mV; $\Delta E_p = 65 \pm 3$ mV for ferrocenium/ferrocene couple) reactions, the subsequent steps are, in general, either quasi-reversible ($E_{pa} - E_{pc} = 90-200$ mV and $i_{pc}/i_{pa} = 0.5-0.8$ in the scan rate (ν) range 100-500 mV s⁻¹) or totally irreversible. The peaks occurring at anodic potentials are ascribed to successive one-electron oxidations of the porphyrin parts of AQ-(H_2)₂ and AQ-(Zn)₂. As seen in Figure 4, the differential pulse voltammograms of AQ-(H_2)₂ and AQ-(Zn)₂ in CH_2Cl_2 contains three reduction peaks corresponding to the reduction of porphyrins (H₂/Zn)/anthraquinone moiety. Comparing the reduction potentials of

$\text{AQ-(H}_2)_2$ and AQ-(Zn)_2 with its reference compounds AQ , H_2L^1 and ZnL^1 , it was found that the reduction potentials for the first peak purely belongs to the reduction of anthraquinone part of both the triads. The second reduction belongs to the first reduction of porphyrin moiety and third reduction peak belongs to the second reduction of porphyrin and anthraquinone of the $\text{D}_2\text{-A}$ systems.

The spectroscopic and electrochemical features described above suggested that in the ground state electronic communication between porphyrin and anthraquinone chromophores is quite negligible in these new D-A systems. More importantly, one can exploit the excited state properties by selective excitation of the individual chromophore units.

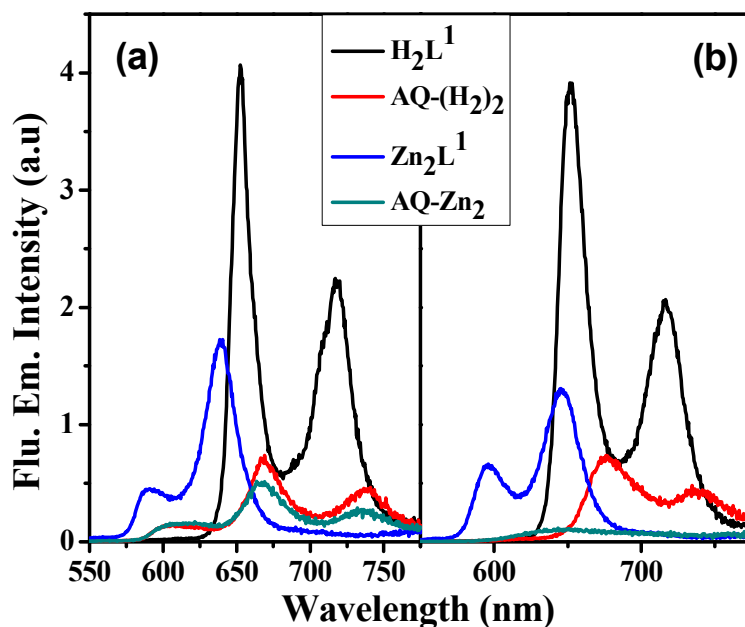


Figure 5: Fluorescence spectra ($\lambda_{\text{ex}} = 420$ nm) of equiabsorbing solutions of H_2L^1 , ZnL^1 , $\text{AQ-(H}_2)_2$ and AQ-(Zn)_2 ($\text{OD } \lambda_{\text{ex}} = 0.05$) in cyclohexane (a) and CH_2Cl_2 (b).

3.2. Singlet state properties.

Figure 5 illustrates the steady state fluorescence spectra of $\text{AQ-(H}_2)_2$ and AQ-(Zn)_2 triads along with their individual constituents H_2L^1 and ZnL^1 measured in cyclohexane and dichloromethane (CH_2Cl_2). Corresponding emission maxima and quantum yields have been collected in Table 2. The fluorescence emission maxima of free base $\text{AQ-(H}_2)_2$ and AQ-(Zn)_2 are red-shifted ~ 25 nm and ~ 4 nm, respectively with respect to isolated free base

porphyrin and zinc porphyrin units. A similar red-shift in emission maxima was also observed in other pyrrole- β substituted porphyrins.^{34,35} The red-shift of these triads is due to the more polar nature of the emitting state originated from the donor-acceptor-donor (D-A-D) type molecular arrangement in which the anthraquinone is acceptor and porphyrin acts as donor. Interestingly, we observe remarkable decrease in porphyrin emission intensity when equiabsorbing solutions of triads were excited at 420 nm (λ_{max} , where porphyrin absorbs predominantly). The possibility of self-aggregation of porphyrins which leads to quenching of fluorescence intensity (as a result of non radiative path in the excited state) can be ruled out as all experiments were carried out with very dilute solutions (10^{-6} M). Moreover, we could not observe substantial changes in the absorption spectra as it happens in few porphyrin systems.³⁷

Table 2: Fluorescence data.^a

Compound	$\lambda_{\text{em}}, \text{nm} (\phi, \%Q)^b$			
	Cyclohexane	Toluene	CH ₂ Cl ₂	CH ₃ CN
	$\lambda_{\text{ex}} = 420 \text{ nm}$			
H₂L¹	653, 719 (0.122)	653, 719 (0.137)	652,716 (0.130)	651,716 (0.130)
ZnL¹	595, 642 (0.037)	598, 647 (0.046)	646, 596 (0.036)	657, 603 (0.048)
AQ-(H₂)₂	671, 742 (0.044, 64)	674, 740 (0.042, 69)	676,738 (0.035, 75)	675, 737 (0.015, 89)
AQ-(Zn)₂	670,737 (0.020,51)	674, 737 (0.022, 52)	651 (0.005, 86)	675, 739 (0.004, 92)

^aError limits: $\lambda_{\text{ex}}, \pm 2 \text{ nm}$, $\phi \pm 10\%$. ^b Q is defined in equation 2 (see text).

The excited state energy transfer (EET) or photoinduced electron transfer (PET) could also be responsible for the decrease in fluorescence intensity. For EET, the emission spectra of donor has to be well matched with absorption of the acceptor. It is evident from the Figures 3 & 5 that the EET is not possible between anthraquinone and porphyrin due to lack of proper spectral overlap. Alternative pathway for emission quenching is the intramolecular PET from the singlet state of porphyrin donor to the ground state of anthraquinone acceptor.

The E_{0-0} (0-0 spectroscopic transition energy) values of porphyrin part of triads, 1.86 ± 0.05 eV, 1.96 ± 0.05 eV for **AQ-(H₂)₂** and **AQ-(Zn)₂** respectively as estimated from overlap of their absorption and emission spectra were found to be in the same range as the E_{0-0} values of free **H₂L¹/ZnL¹**.³⁸ The change in free energy for PET from the porphyrin to the anthraquinone can be calculated using the equation,

$$\Delta G(^1\text{Por} \rightarrow \text{AQ}) = E_{\text{CT}}(\text{Por}^+ \text{AQ}^-) - E_{0-0}(\text{Por}) \quad (1)$$

ΔG was found to be -0.096 & -0.24 eV for **AQ-(H₂)₂** & **AQ-(Zn)₂** respectively, when excited at 420 nm. This ΔG clearly indicates that there could be a possibility of PET from free base/metal porphyrin to anthraquinone.

Fluorescence quantum yields of the triads and individual constituents have been estimated (Table 2) by comparing the emission curves of reference compounds (*i.e.*, **H₂L¹** or **ZnL¹**, $\phi = 0.13 \pm 0.01$ and 0.036 ± 0.001 , respectively in CH_2Cl_2 solvent) with that of triads. It was found that the fluorescence quantum yield (ϕ) of **AQ-(H₂)₂** and **AQ-(Zn)₂** are 0.042 and 0.022 respectively in CH_2Cl_2 solvent. The quenching efficiency values (Q) can be estimated from,

$$Q = \frac{\phi(\text{H}_2\text{L}^1)\text{or}(\text{ZnL}^1) - \phi[\text{AQ}-(\text{H}_2)_2]\text{or}[\text{AQ}-(\text{Zn})_2]}{\phi(\text{H}_2\text{L}^1)\text{or}(\text{ZnL}^1)} \quad (2)$$

Where $\phi(\text{H}_2\text{L}^1)/(\text{ZnL}^1)$ and $\phi(\text{AQ}-(\text{H}_2)_2)/\text{AQ}-(\text{Zn})_2$ refer to the fluorescence quantum yields of **H₂L¹/ZnL¹** and the triads respectively; ($\lambda_{\text{ex}} = 420$ nm). As the static dielectric constant of the solvent is increased, the fluorescence quantum yield decreased gradually (Table 2), indicate the excited state electron transfer mechanism. For example, quenching efficiencies in cyclohexane and toluene are less compared to the CH_2Cl_2 and CH_3CN . In general, the PET process is accelerated by polar solvents than the non-polar solvents, so the present results are in consistent with the literature.³⁹ Efficient quenching of the **AQ-(Zn)₂** triad relative to that of the **AQ-(H₂)₂** can be directly attributed to the more exothermic value of ΔG_{PET} of **AQ-(Zn)₂**.

Further evidence of the intramolecular PET process has been evaluated by measuring the excited state decay curves. Figure 6 illustrates excited state decay curves of triads, collected in CH_2Cl_2 solvent upon excitation at 405 nm and the decay parameters collected in four different solvents are shown in Table 3. From the data, it is clear that the fluorescence

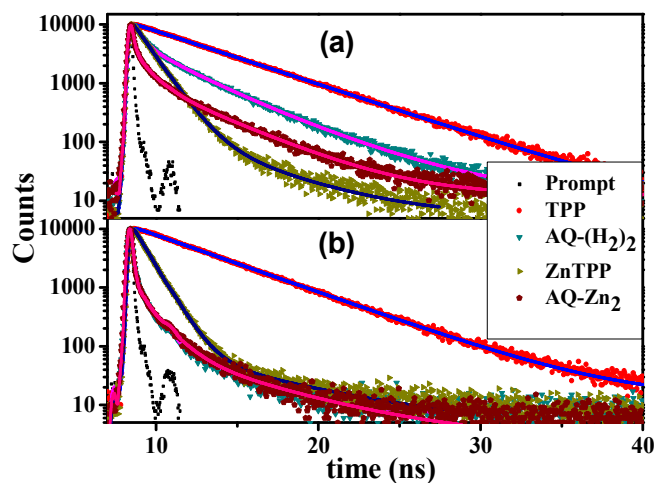


Figure 6: Fluorescence decay ($\lambda_{\text{ex}} = 405 \text{ nm}$, $\lambda_{\text{em}} = 650 \text{ nm}$) in cyclohexane (a) and CH_2Cl_2 (b).

Table 3: Fluorescence decay parameters[†] and electron transfer rate constants (k_{ET} , S^{-1}).[‡]

Compound	$(\tau, \text{ns (A\%)}, k_{\text{ET}}, \text{s}^{-1})$			
	Cyclohexane	Toluene	CH_2Cl_2	CH_3CN
H_2L^1	9.47	9.71	8.81	9.40
ZnL^1	1.93(93)	2.07(95)	1.76(95)	1.72(89)
	2.07(7)	1.11(5)	1.17(5)	2.86(11)
$\text{AQ-(H}_2)_2$	1.07(44)	3.08(57)	0.13(66) [§]	0.69 (57)
	9.12(35)	9.26(23)	6.36(12.0)	7.60 (32)
	5.14(21)	4.60 (20)	1.57(22)	2.28 (11)
	8.3×10^8	2.2×10^8	7.6×10^9	1.3×10^9
AQ-Zn_2	1.60(85)	1.48(68)	0.33(65) [§]	0.60(51)
	1.16(6)	2.04(11)	2.46(13)	1.82(26)

	0.57(9)	0.29(21) [§]	1.22(22)	1.00(23)
	1.0×10^8	1.9×10^8	2.4×10^9	1.1×10^9

† All lifetimes are in nanoseconds (ns). ‡ Error limits of τ and $k_{ET} \sim 10\%$. Values in parenthesis are relative amplitude of corresponding decay component. § These short lifetime components are limited by the instrument response function (IRF).

lifetimes, τ ($\lambda_{ex} = 405$ nm and $\lambda_{em} = 650$ nm) of both **AQ-(H₂)₂** and **AQ-(Zn)₂** are decreased in all solvents when compared to **H₂L¹/ZnL¹**. In all solvents, **AQ-(H₂)₂** decay curves are fitted with a tri-exponential expression and major component is having shorter lifetime which is attributed to the deactivation (quenching) of the excited porphyrin by anthraquinone.¹⁷ The other two lifetime components are assigned either to an unquenched decay or decay of the porphyrin-hydroquinone generated by porphyrin sensitized photoreduction⁴⁰ and different conformers of the molecule with flexible linker in solution-state^{41,42}. On the other hand, **AQ-(Zn)₂** decay curves are fitting into a three-exponential expression composed of one major (see table 3, shorter lifetime) component and two minor components (shorter and longer lifetime). From this data, the shorter lifetime with higher amplitude and longer lifetime components have the same origin as in **AQ-(H₂)₂**, but the additional shorter lifetime component may be due to the non-covalent interaction of oxygen lone pair of electrons (anthraquinone) with zinc metal present in other porphyrin of **AQ-(Zn)₂**. We believe that this anthraquinone-ligated state is responsible for the additional short-lived component obtained from the TCSPC experiments.¹⁷ In all four investigated solvents, it is observed that the shorter lifetime of **AQ-(H₂)₂** have much larger amplitudes relative to the longer lifetime components. Similar features are also seen in **AQ-(Zn)₂** triad.

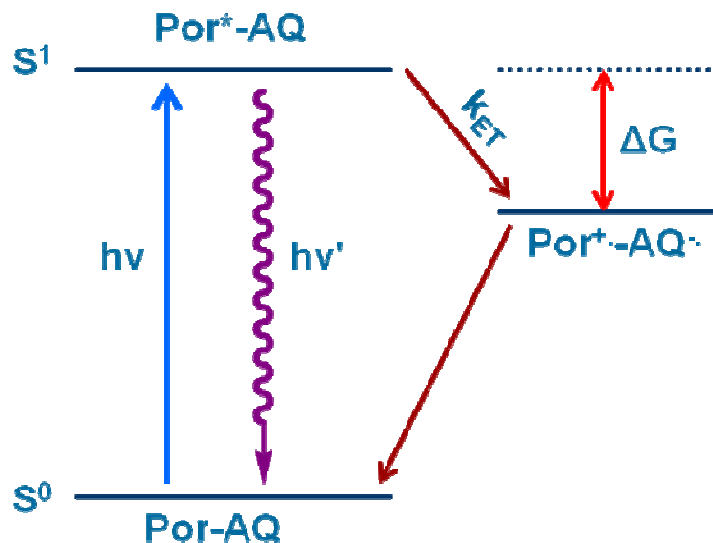
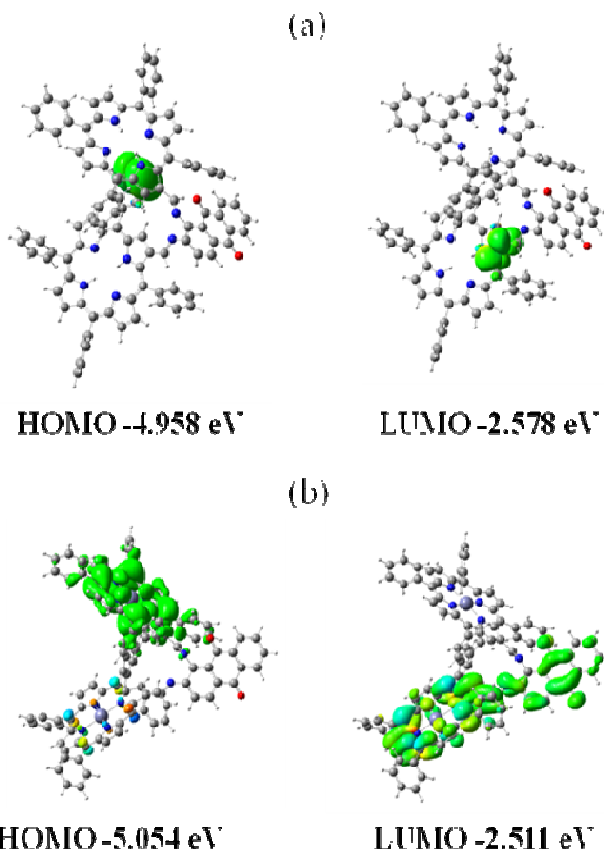


Figure 7: Photoinduced electron-transfer scheme of bis-porphyrin-anthraquinone triads.

Further, rate constant (k_{ET}) for the charge transfer state Por^+AQ^- have been calculated using eq (3) and summarized in Table 3.

$$k_{ET} = (1/\tau_f) - k \quad (3)$$

Where k is the reciprocal of the lifetime of the $\text{H}_2\text{L}^1/\text{ZnL}_1$, τ_f is the lifetime of $\text{AQ}-(\text{H}_2)_2/\text{AQ}-(\text{Zn})_2$. The solvent-dependent k_{ET} values are in the range of 1.0×10^8 to $7.7 \times 10^9 \text{ s}^{-1}$. The observed general increase of the k_{ET} values with increasing polarity of the solvent is consistent with the participation of a charge transfer state in the excited state deactivation of the porphyrin components of these $\text{D}_2\text{-A}$ systems. Figure 7 shows the energy levels of the porphyrin singlet excited state and the charge transfer state that participates in the PET processes in bisporphyrin–anthraquinone triads. In order to establish the intramolecular PET process of these two triads, we have carried out computational calculations to generate frontier molecular orbitals of both triads.



33 **Figure 8:** Frontier molecular orbitals, HOMO and LUMO of a) AQ-(H₂)₂ and b) AQ-(Zn)₂
34 optimized at the B3LYP/6-31G(d) level.

36 3.3. Theoretical calculations.

37
38
39 In general, intramolecular electron transfer operates either *through-space* or *through-*
40 *bond* mechanism. In the former mechanism, (*through space*) electron transfer occurs from
41 HOMO (the highest occupied molecular orbital) of the donor moiety to LUMO (the lowest
42 unoccupied molecular orbital) of acceptor moiety when they are in close proximity and
43 (depends strongly) on the orientation of donor and acceptor moieties.⁴³⁻⁴⁴ The later
44 mechanism (*through bond*) is rather less sensitive to geometrical position/orientation of
45 donor and acceptor moieties but strongly depends on the number of atoms connecting them.
46 In this case, electronic states of spacer (moieties between the donor and the acceptor) will
47 mix with those of the donor and acceptor, thus the *through-bond* mechanism is synonymous
48 with superexchange.^{45,46} In order to examine the nature and position of frontier molecular
49 orbitals, density functional theory (DFT) calculations have been carried. Complete
50
51
52
53
54
55
56
57
58
59
60

1
2
3 optimization without any constraint was done using B3LYP and 6-31g(d) basis set to see the
4 structural parameters of the two systems, **AQ-(H₂)₂** and zinc **AQ-(Zn)₂**.
5
6

7 Figure 8 displays the HOMO and LUMO distribution and geometrical optimized
8 structures of the triads **AQ-(H₂)₂** and **AQ-(Zn)₂**, obtained by DFT calculations. From Figure
9 8, it is clear that the HOMO is mainly distributed at porphyrin moiety while LUMO mainly
10 distributed at anthraquinone moiety. The energies of HOMO and LUMO for triads **AQ-(H₂)₂**
11 and **AQ-(Zn)₂** were found to be -4.958 & -5.054 eV and -2.578 & -2.511 eV, respectively.
12 From the geometrical optimized structures (Fig.8), the two porphyrin rings are away from
13 each other as the connecting bonds between porphyrin ring and anthraquinone moieties are
14 not long enough to have π - π interaction. Similarly, the porphyrin and anthraquinone rings
15 are also far apart which clearly suggest that there is very less chance to have facial interaction
16 between donor porphyrin and acceptor anthraquinone. Moreover, phenyl rings at *-meso*
17 positions are found to be perpendicular to the plane of porphyrin ring, which prevent the
18 stacking interaction. (All these observations corroborate the prevalence of *through-bond*
19 intramolecular electron transfer mechanism in the current systems). As discussed in earlier
20 sections, the fluorescence quantum yields, lifetimes, and electron transfer rates of these triads
21 are found to be strongly dependent on solvent polarity. One cannot expect this solvent
22 dependency if electron transfer occurs *through-space* mechanism. Therefore the results are
23 best compatible with "*through-bond*" mechanism for electron transfer pathway.
24
25
26
27
28
29
30
31
32
33
34
35

36 4. Conclusions

37
38
39 In conclusion, bisporphyrin-anthraquinone triads having azomethine-bridge at
40 pyrrole- β position of porphyrin macrocycle were successfully shown to be a model
41 photosynthetic reaction center to simulate the electron transfer from chlorophylls to the
42 electron acceptors. The ground state properties indicate that there are no interactions between
43 porphyrin macrocycles and anthraquinone moieties in both the triads. Steady-state and time-
44 resolved spectroscopy showed that **AQ-(H₂)₂** and **AQ-(Zn)₂** undergo rapid intramolecular
45 electron transfer from singlet state of porphyrin to anthraquinone. The electron transfer rates
46 are found in the range 1.0×10^8 to 7.7×10^9 s⁻¹ and are solvent dependent.
47
48
49
50
51
52
53
54
55
56
57
58
59
60

Acknowledgement

We are grateful to Department of Science and Technology (DST, SR/S1/IC21/2008) for financial support of this work. One of the authors PS is thankful to CSIR for the fellowship. YS thank BRNS (DAE) for financial support.

Supporting Information

Characterization data of the compounds such as IR spectra (Figure S1 & S2), ¹H NMR (Figures S3, S4, S5 & S6) and MALDI-MS spectra (Figure S7 & S8), absorption spectra of AQ-(H₂)₂ in different solvents (Figure S9), fluorescence behaviour of the compounds in toluene and acetonitrile (Figure S10 & S11), fluorescence decay curves (Figure S12 & S13) and optimized geometries of molecules (Figure S14) are available free of charge via the Internet at <http://pubs.acs.org>.

References and notes

1. Kim, J. H.; Lee, M.; Lee, J. S.; Park, Ch. B. Self-Assembled Light-Harvesting Peptide Nanotubes for Mimicking Natural Photosynthesis. *Angew. Chem. Int. Ed.* **2012**, *51*, 517-520.
2. McConnell, I.; Li, G.; Brudvig, G. W. Energy Conversion in Natural and Artificial Photosynthesis. *Chem. Biol.* **2010**, *17*, 434-447.
3. Gust, D.; Moore, T. A.; Moore, A. L. Solar Fuels via Artificial Photosynthesis. *Acc. Chem. Res.* **2009**, *42*, 1890-1898.
4. D'Souza, F.; Smith, P. M.; Zandler, M. E.; McCarty, A. L.; Ito, M.; Araki, Y.; Ito, O. Energy Transfer Followed by Electron Transfer in a Supramolecular Triad Composed of Boron Dipyrin, Zinc Porphyrin, and Fullerene: A Model for the Photosynthetic Antenna-Reaction Center Complex. *J. Am. Chem. Soc.*, **2004**, *126*, 7898-7907.
5. Balzani, V.; Bolletta, F.; Gandolfi, M. T.; Maestri, M. Excited States Redox Reactions *Topics in Current Chemistry* **1978**, *75*, 1-64.
6. Wiehe, A.; Senge, M. O.; Schafer, A.; Speck, M.; Tannert, S.; Kurreck, H.; Roder, B. Electron Donor-Acceptor Compounds: Exploiting the Triptycene Geometry for the Synthesis of Porphyrin Quinone Dyads, Triads, and a Tetrad. *Tetrahedron* **2001**, *57*, 10089-10110.
7. Koyama, Y.; Miki, T.; Wang, X. -F.; Nagae, H. Dye-Sensitized Solar Cells Based on the Principles and Materials of Photosynthesis: Mechanisms of Suppression and Enhancement of Photocurrent and Conversion Efficiency. *Int. J. Mol. Sci.* **2009**, *10*, 4575-4622.

8. Bai, D.; Beeniston, A. C.; Hagon, J.; Lemmetyinen, H.; Tkachenko, N. V.; Clegg, W.; Harrington, R. W.; Exploring Förster Electronic Energy Transfer in a Decoupled Anthracenyl-Based Borondipyrromethene (BODIPY) Dyad. *Phys. Chem. Chem. Phys.* **2012**, *14*, 4447-4456.
9. Liu, J. Y.; El-Kously, M. E. E. -L.; Fukuzumi, S.; Ng, D. K. P. Mimicking Photosynthetic Antenna-Reaction-Center Complexes with a (Boron Dipyrromethene)₃-Porphyrin-C₆₀ Pentad *Chem. Eur. J.* **2011**, *17*, 1605-1613.
10. Vijendra, S. S.; Mangalampalli, R. Supramolecular Tetrads Containing Sn(IV) Porphyrin, Ru(II) Porphyrin, and Expanded Porphyrins Assembled Using Complementary Metal-Ligand Interactions. *Inorg. Chem.* **2011**, *50*, 1713-1722.
11. Jing, B.; Zhu, D. Fullerene-Fluorescein-Anthracene Hybrids: A Model for Artificial Photosynthesis and Solar Energy Conversion. *Tetrahedron Letters* **2004**, *45*, 221-224.
12. Flamigni, L.; Talarico, A.; Gunter, M. J.; Johnston, M. R.; Jaynes, T. P. Photoinduced Electron Transfer in Paraquat Inclusion Complexes of Porphyrin-Based Receptors. *New J. Chemistry* **2003**, *27*, 551-559.
13. Flamigni, L.; Johnston, M. R. Giribabu, L. Photoinduced Electron Transfer in Bisporphyrin-Diimide Complexes. *Chem. Eur. J.* **2002**, *8*, 3938-3947.
14. Jono, R.; Yamashita, K. Two Different Lifetimes of Charge Separated States: A Porphyrin-Quinone System in Artificial Photosynthesis. *J. Phys. Chem. C* **2012**, *116*, 1445-1449.
15. Zhao, P.; Huang, J. -W.; Xu, L. -C.; Ma, L.; Ji, L. -N. The Photoinduced Electron Transference of Porphyrin-Anthraquinone Dyads Bridged with Different Lengths of Links. *Spectrochimica Acta Part A*, **2011**, *78*, 437-442.
16. Tao, M.; Liu, L.; Liu, D.; Zhou, X. Photoinduced Energy and Electron Transfer in Porphyrin-Anthraquinone Dyads Bridged with a Triazine Group. *Dyes & Pigments* **2010**, *85*, 21-26.
17. Kumar, P. P.; Premaladha, G.; Maiya, B. G. Porphyrin-Anthraquinone Dyads: Synthesis, Spectroscopy and Photochemistry. *J. Chem. Sci.* **2005**, *117*, 193-201.
18. Williams, D. A.; Bowler, B. E. Porphyrin to Quinone Electron Transfer Across a Dipeptide which Forms an α -Helical Turn. *Inorganica Chimica Acta* **2000**, *297*, 47-55.
19. Shibano, Y.; Sasaki, M.; Tsuji, H.; Araki, Y.; Ito, O.; Tamao, K. Conformation Effect of Oligosilane Linker on Photoinduced Electron Transfer of Tetrasilane-Linked Zinc Porphyrin-[60]Fullerene Dyads. *J. Organometallic Chemistry*, **2007**, *692*, 356-367.
20. Marcus, R. A. Electron Transfer Reactions in Chemistry: Theory and Experiment. *Angew. Chem. Int. Ed.* **1993**, *32*, 1111-1121.
21. Schuster, D. I.; MacMahon, S.; Guldi, D. M.; Echegoyen, L.; Braslavsky, S. E. Synthesis and photophysics of porphyrin-fullerene donor-acceptor dyads with conformationally flexible linkers. *Tetrahedron* **2006**, *62*, 1928-1936.

- 1
2
3 22. Okamoto, K.; Fukuzumi, S. Hydrogen Bonds Not Only Provide a Structural Scaffold to
4 Assemble Donor and Acceptor Moieties of Zinc Porphyrin–Quinone Dyads but Also
5 Control the Photoinduced Electron Transfer to Afford the Long-Lived Charge-Separated
6 States. *J. Phys. Chem. B* **2005**, *109*, 7713-7723.
7
- 8 23. Wasielewski, M. R. Photoinduced Electron Transfer in Supramolecular Systems for
9 Artificial Photosynthesis. *Chem. Rev.* **1992**, *92*, 435-461.
10
- 11 24. Kandhadi, J.; Kanaparthi, R. K.; Giribabu, L. Germanium(IV) Phthalocyanine-Porphyrin
12 Based Hetero Trimers: Synthesis, Spectroscopy and Photochemistry.
13 *J. Porphyrins & Phthalocyanines* **2012**, *16*, 282-289.
14
- 15 25. Giribabu, L.; Kumar, C. V.; Reddy, P. Y. Axial-Bonding Heterotrimers Based on
16 Tetrapyrrolic Rings: Synthesis, Characterization, and Redox and Photophysical
17 Properties. *Chem. Asian J.* **2007**, *2*, 1574-1580.
18
- 19 26. Reeta, P. S.; Kanaparthi, R. K.; Giribabu L. β -Pyrrole Substituted Porphyrin-Pyrene
20 Dyads Using Vinylene Spacer: Synthesis, Characterization and Photophysical Properties.
21 *J. Chem. Sci.* **2013**, *125*, (0000).
22
- 23 27. Fuhrhop, J. H.; Smith, K. M. In *Porphyrins and Metalloporphyrins*, Smith KM. (Ed.)
24 Elsevier: Amsterdam, **1975**, 769.
25
- 26 28. Bonfantini, E. E.; Burrell, A. K.; Campbell, W. M.; Crossley, M. J.; Gosper, J. J.;
27 Harding, M. M.; Officer, D. L.; Reid, D. C. W. Efficient synthesis of Free-Base 2-
28 Formyl-5,10,15,20-Tetraarylporphyrins, Their Reduction and Conversion to [(Porphyrin-
29 2-yl)methyl]phosphonium Salts. *J. Porphyrins & Phthalocyanines* **2002**, *6*, 708-719.
30
- 31 29. Giribabu, L.; Kumar, C. V.; Reddy, V. G.; Reddy, P. Y.; Rao, Ch. S.; Jang, S. -R.; Yum,
32 J. -H.; Nazeeruddin, M. K.; Gratzel, M. Unsymmetrical Alkoxy Zinc Phthalocyanine for
33 Sensitization of Nanocrystalline TiO₂ Films. *Sol. Energy Mater. Sol. Cells* **2007**, *91*,
34 1611-1617.
35
- 36 30. Gaussian 09 Revision A.01, Frisch, M. J.; Trucks, G. W.; Schlegel, H. B.; Scuseria, G. E.;
37 Robb, M. A.; Cheeseman, J. R.; Scalmani, G.; Barone, V.; Mennucci, B.; Petersson, G. A.
38 et al. *Gaussian, Inc., Wallingford CT*, **2009**.
39
- 40 31. Quimby, D. J.; Longo, F. R. Luminescence Studies on Several Tetraarylporphyrins and
41 Their Zinc Derivatives. *J. Am. Chem. Soc.* **1975**, *97*, 5111-5117.
42
- 43 32. Rodriguez, J.; Kirmaier, C.; Holten, D. Optical Properties of Metalloporphyrin Excited
44 States. *J. Am. Chem. Soc.*, **1989**, *111*, 6500-6506.
45
- 46 33. Fukuzumi, S.; Endo, Y.; Kashiwagi, Y.; Araki, Y.; Ito, O.; Imahori, H. Novel
47 Photocatalytic Function of Porphyrin-Modified Gold Nanoclusters in Comparison with
48 the Reference Porphyrin Compound. *J. Phys. Chem. B*, **2003**, *107*, 11979-11986.
49
- 50 34. Reeta, P. S.; Kandhadi, J.; Giribabu, L. One-pot Synthesis of β -Carboxy Tetra Aryl
51 Porphyrins: Potential Applications to Dye-Sensitized Solar Cells. *Tetrahedron Letts.*,
52 **2010**, *51*, 2865-2867.
53
- 54 35. Giribabu, L.; Kumar, C. V.; Reddy, P. Y. Porphyrin-Rhodanine Dyads for Dye Sensitized
55 Solar Cells. *J. Porphyrins & Phthalocyanines*, **2006**, *10*, 1007-1016.
56
57
58
59
60

- 1
2
3 36. James R. Bolton, J. R.; Ho, T.-F.; Liauw, S.; Aleksander Siemiarzczuk, A.; Calvin S. K.
4 Wan, C. S. K.; Weedon, A. C. Light-induced Intramolecular Electron Transfer from a
5 Porphyrin linked to a *p*-Benzoquinone by a Rigid Spacer Group. *J. Chem. Soc., Chem.*
6 *Commun.*, **1985**, 559-560, and references therein.
7
8
9 37. Barber, D.C.; Freitag, R.A.; Whitten, D.G. Atropisomer-specific formation of premicellar
10 porphyrin J-aggregates in aqueous surfactant solutions. *J. Phys. Chem.*, **1991**, 95, 4074-
11 4086.
12
13 38. Excited state singlet state energy levels ($E_{0,0}$) of H_2L^1 , ZnL^1 , $AQ-(H_2)_2$ and $AQ-(Zn)_2$
14 and are 1.96, 2.05, 1.85 and 1.96 eV, respectively.
15
16 39. Bolton, J. R.; Schmidt, J. A.; Ho, T. F.; Liu, J. -Y.; Roach, K. R.; Weedon, A. C.; Archer,
17 M. D.; Wilford, J. H.; Gadzekpo, V. P. Y. Electron transfer in Inorganic, Organic and
18 Biological Systems. *American Chemical Society*, **1991**, Chapter 7.
19
20 40. Korth, O.; Wiehe, A.; Kurreck, H.; Roder, B. Photoinduced Intramolecular Electron
21 Transfer in Covalently Linked porphyrin-Triptycene-Bis/quinone Diads and Triads.
22 *Chemical Physics*, **1999**, 246, 363-372.
23
24 41. Brookfield, R. L.; Ellul, H.; Harriman, A.; Porter, G. Luminescence of Porphyrins and
25 Metalloporphyrins. Part 11.- Energy Transfer in Zinc-Metal-Free Porphyrin Dimers. *J.*
26 *Chem. Soc. Faraday Trans. 2*, **1986**, 82, 219-233.
27
28 42. Sakata, Y.; Nishitani, S.; Nishimizu, N.; Misumi, S. Synthesis of a Model Compound
29 for the Photosynthetic Electron Transfer. *Tetrahedron Lett.*, **1985**, 26, 5207-5210.
30
31 43. Karr, P. A.; Zandler, M. E.; Beck, M.; Jaeger, J. D.; McCarty, A. L.; Smith, P. M.;
32 D'Souza, F. Predicting the Site of Electron Transfer Using DFT Frontier Orbitals:
33 Studies on Porphyrin Attached Either to Quinone or Hydroquinone, and Quinhydrone
34 Self-Assembled Supramolecular Complexes. *J. Mol. Struct. Theochem.* **2006**, 765, 91-
35 103.
36
37 44. Paddon-Row, M. N. Some Aspects of Orbital Interactions Through Bonds: Physical and
38 Chemical Consequences. *Acc. Chem. Res.* **1982**, 15, 245-251.
39
40 45. Anderson, P. W. Antiferromagnetism. Theory of Superexchange Interaction. *Phys. Rev.*
41 **1950**, 79, 350-356.
42
43 46. Won, Y.; Friesner, R. A. On the Viability of the Superexchange Mechanism in the
44 Primary Charge Separation Step of Bacterial Photosynthesis. *Biochim. Biophys. Acta*
45 *Bioenerg.* **1988**, 935, 9-18.
46
47
48
49
50
51
52
53
54
55
56
57
58
59
60

Bis-Porphyrin-Anthraquinone Triads: Synthesis, Spectroscopy and Photochemistry

L. Giribabu^{*,a}, P. Silviya Reeta^a, Ravi Kumar Kanaparthi^a, Malladi Srikanth^b, Y. Soujanya^b

Table of Contents

